Designing Affine OCDM Systems with Maximum Diversity

Sidong Guo, *Student Member, IEEE*, Xiaoli Ma, *Fellow, IEEE,* and Yiyin Wang, *Senior Member, IEEE*

***Abstract*—This work considers the problem of enabling maximum multipath diversity of orthogonal chirp division multiplexing (OCDM)-based systems. We define and study an Affine OCDM (A-OCDM) system in which a chirp parameter is adapted to enable maximum diversity offered by frequency selective channels. Our proposed system also reduces implementation complexity by eliminating the need for precoding, compared to linear constellation precoded OCDM. Corroborating simulations are provided to show that A-OCDM also preserves OCDM systems' resilience against interference offered by spreading.**

***Index Terms*—OCDM, diversity, linear constellation precoding (LCP), algebraic number theory**

I. Introduction

DIVERSITY techniques continue to be effective measures in mitigating the challenges posed by severe channel impairments. To enhance multipath diversity offered by frequency-selective channels, input constellation symbols can be rotated with complex phasors, thereby creating signal space diversity in the received symbols [1]. Chief among the many strategies to enable maximum diversity for wireless systems is the linear constellation precoding (LCP) approach, which seeks to maximize multipath diversity by using a judiciously designed constellation precoder [2] [3]. For instance, linear constellation precoded orthogonal frequency division multiplexing (LCP-OFDM) systems enable maximum diversity with maximum likelihood estimator (MLE) [2], compared to its unprecoded counterpart that enables only unit diversity.

The objective of the present work is to further the understanding of diversity analysis to the newly emerged orthogonal chirp division multiplexing (OCDM) systems. OCDM represents a chirp-based approach to the design of multicarrier kernel, where each subchirp is spread across the entire band via the Fresnel transform, thereby offering improved resilience to narrow band interferences (NBIs) and time burst interferences (TBIs) [4]. The precoding introduced by the Fresnel transform contributes to OCDM systems having superior bit error rate (BER) performance over frequency-selective channels, compared to OFDM. Nevertheless, a notable limitation is that uncoded OCDM only enables unit diversity with MLE [4]. Despite extensive results in related areas such as multi-user systems and performance analysis [4], [5], algorithms to enable full diversity of OCDM-based systems remain an area that has received comparatively less attention. Preliminary result has shown that LCP techniques can be applied to remedy this limitation, authors in [5] demonstrated linear constellation precoded OCDM (LCP-OCDM) retains the same diversity performance as LCP-OFDM.

We propose and evaluate an alternative OCDM-based system, namely Affine OCDM (A-OCDM), to LCP-OCDM system that enjoys reduced complexity while enabling maximum diversity. Our approach relies on Fresnel transform being a special case of discrete affine Fourier transform (DAFT). Existing researches have demonstrated that DAFT-based multicarrier system can adapt DAFT parameters to be more robust against Doppler effects [6] [7]. More recently, in the context of a doubly-selective channel, authors in [8] demonstrated that DAFT parameters can be adapted to achieve a full delay-Doppler representation of the channel. In a parallel vein to these results, A-OCDM extends the OCDM model in [9] by selecting appropriate chirp parameters based on the blocksize. As a result, A-OCDM does not require additional precoding while enable same maximum diversity as LCP-OCDM. In addition, we also show through simulations that A-OCDM retains same resilience against NBIs.

Notations: Uppercase bold letters are used to represent matrices, and $[\mathbf{A}]_{k,n}$ denotes the k-th row and n-th column element of the matrix $\mathbf{A}$. Lowercase bold letters are used to denote column vectors, and $[\mathbf{a}]_k$ is the k-th element of column vector $\mathbf{a}$. In particular, we employ the notation convention that first element of matrix/column vector is the 0-th element. Let $(.)^T$ and $(.)^{\mathcal{H}}$ represent transpose and conjugate transpose respectively. Blackboard letters denotes a set, $\mathbb{R}$, $\mathbb{C}$, $\mathbb{Q}$, $\mathbb{Z}$, $\mathbb{N}$ denote the set of real, complex, rational, integer and natural numbers respectively. The ring of Gaussian integers is denoted as $\mathbb{Z}(j)$, where j is the imaginary unit. Let $\psi(x)$ be the Euler totient function of x and $R(\mathbf{A})$ be the rank of a matrix $\mathbf{A}$. Finally, l_2 norm is denoted as $||.||$, and the circularly symmetric complex Gaussian random variable x with mean μ and variance σ^2 is represented as $x \sim \mathcal{CN}(\mu, \sigma^2)$.

II. System Model and Performance Metrics

We first present the A-OCDM system model. This is followed up by establishing the definitions of diversity, as relevant to the proposed system.

A. Affine OCDM System Model

Consider an OCDM-based multicarrier system where information-carrying symbols are chosen from the ring of Gaussian integers (quadrature amplitude modulation (QAM) or pulse amplitude modulation (PAM)). Let $\mathbf{s} \in \mathbb{Z}(j)^{N\times 1}$ be the $N \times 1$ symbol vector defined as $\mathbf{s} = [s_1, \ldots, s_N]^T$, where we make the practical assumption that block size N is an exponent of 2 $(i.e., N = 2^z, z \in \mathbb{Z}^+)$ for the rest of the paper. The symbol vector is transformed to the time domain

as $\mathbf{x} = \mathbf{\Phi}_b^{\mathcal{H}}\mathbf{s}$, where $\mathbf{\Phi}_b$ is the $N \times N$ matrix with elements defined as [1]

$$[\mathbf{\Phi}_b]_{m,n} = \frac{1}{\sqrt{N}} e^{-j\frac{\pi}{4}} \times e^{j2\pi(bm^2 - \frac{1}{N}mn + \frac{1}{2N}n^2)}. \quad (1)$$

The matrix $\mathbf{\Phi}_b$ can be expressed as a concatenation of three invertible matrices, along with a constant term as $\mathbf{\Phi}_b = e^{-j\frac{\pi}{4}}\mathbf{\Lambda}_b\mathbf{F}\mathbf{\Lambda}_{\frac{1}{2N}}$, where $\mathbf{F}$ is the $N \times N$ normalized discrete Fourier transform (DFT) matrix defined as $[\mathbf{F}]_{m,n} = \sqrt{1/N}e^{-j2\pi mn/N}$. The $N \times N$ diagonal matrix $\mathbf{\Lambda}_b$ parameterized by b has diagonal elements defined as

$$[\mathbf{\Lambda}_b]_{m,m} = e^{j2\pi bm^2},$$

and $\mathbf{\Lambda}_{\frac{1}{2N}}$ is a diagonal matrix with the same definition as $\mathbf{\Lambda}_b$.

Thereafter, assuming a channel impulse response (CIR) $\mathbf{h} = [h_0, \ldots, h_L]^T$ of order L, a cyclic prefix (CP) of length L is inserted. After removing the CP and applying $\mathbf{\Phi}_b$ at the receiver, the system model over a time-invariant frequency-selective channel is [9] [10]

$$\begin{aligned}\mathbf{y} &= \mathbf{\Phi}_b\mathbf{H}\mathbf{\Phi}_b^{\mathcal{H}}\mathbf{s} + \mathbf{n} \\ &\overset{(\alpha)}{=} e^{j\frac{\pi}{4}}\mathbf{\Phi}_b\mathbf{F}^{\mathcal{H}}\mathbf{F}\mathbf{H}\mathbf{\Lambda}_{\frac{1}{2N}}^{\mathcal{H}}\mathbf{F}^{\mathcal{H}}\mathbf{\Lambda}_{\frac{1}{2N}}^{\mathcal{H}}\mathbf{\Lambda}_{\frac{1}{2N}}\mathbf{\Lambda}_b^{\mathcal{H}}\mathbf{s} + \mathbf{n} \\ &\overset{(\beta)}{=} \mathbf{\Phi}_b\mathbf{F}^{\mathcal{H}}\mathbf{D}\mathbf{\Gamma}^{\mathcal{H}}\mathbf{F}\mathbf{\Lambda}_{\frac{1}{2N}}\mathbf{\Lambda}_b^{\mathcal{H}}\mathbf{s} + \mathbf{n} \\ &= \mathbf{\Phi}_b\mathbf{F}^{\mathcal{H}}\bar{\mathbf{D}}\mathbf{F}\mathbf{\Lambda}_{\frac{1}{2N}}\mathbf{\Lambda}_b^{\mathcal{H}}\mathbf{s} + \mathbf{n}, \end{aligned} \quad (2)$$

where $\mathbf{n} \sim \mathcal{CN}(0, N_0)$. In (2), $\mathbf{H}$ is a circulant matrix with elements defined as $[\mathbf{H}]_{n,m} = h_{(n-m) \bmod N}$, and $\mathbf{D} = \mathbf{F}\mathbf{H}\mathbf{F}^{\mathcal{H}}$ is the frequency domain channel matrix. In addition, $\bar{\mathbf{D}} = \mathbf{D}\mathbf{\Gamma}^{\mathcal{H}}$, and $\mathbf{\Gamma}$ is the $N \times N$ diagonal matrix defined as $[\mathbf{\Gamma}]_{n,n} = [\mathbf{\Lambda}_{\frac{1}{2N}}^{\mathcal{H}}]_{n,n} = e^{-j\frac{\pi}{N}n^2}$. Note that (α) in (2) uses the definition of $\mathbf{\Phi}_b^{\mathcal{H}}$, followed by inserting $\mathbf{\Lambda}_{\frac{1}{2N}}^{\mathcal{H}}\mathbf{\Lambda}_{\frac{1}{2N}}$ between $\mathbf{F}^{\mathcal{H}}$ and $\mathbf{\Lambda}_b^{\mathcal{H}}$, $\mathbf{F}^{\mathcal{H}}\mathbf{F}$ between $\mathbf{\Phi}_b$ and $\mathbf{H}$. In (2), (β) is supported by the property $e^{j\frac{\pi}{4}}\mathbf{\Lambda}_{\frac{1}{2N}}^{\mathcal{H}}\mathbf{F}^{\mathcal{H}}\mathbf{\Lambda}_{\frac{1}{2N}}^{\mathcal{H}} = \mathbf{F}^{\mathcal{H}}\mathbf{\Gamma}^{\mathcal{H}}\mathbf{F}$.

Remark 1: The model defined in (2) differs from the DAFT-based model used in [7], [8], where the constant term $e^{-j\frac{\pi}{4}}$ is not included. In addition, DAFT-based models are governed by two parameters with variable chirp rate. In this regard, our definition of A-OCDM system in (2) captures the modeling assumption in the seminal OCDM literature [9], where the chirp rate $\frac{1}{2N}$ is fixed. Thus, $\mathbf{\Phi}_b$ can be viewed as a modified Fresnel transform, enabling the matrix property $\mathbf{\Phi}_b = \mathbf{\Lambda}_b\mathbf{\Lambda}_{\frac{1}{2N}}^{\mathcal{H}}\mathbf{F}^{\mathcal{H}}\mathbf{\Gamma}\mathbf{F}$, which we rely on to diagonalize the channel.

B. Multipath Diversity

Assuming that perfect channel state information (CSI) is available at the receiver and MLE is employed, the conditional pair-wise error probability (PEP) can be bounded as

$$P(\mathbf{s} \to \mathbf{s}'|\mathbf{h}) \leq \exp\left[-\frac{d^2(\mathbf{y}', \mathbf{y})}{4N_0}\right]. \quad (3)$$

An error event implies $\mathbf{s} \neq \mathbf{s}'$, where $\mathbf{s}, \mathbf{s}' \in \mathbb{Z}(j)^{N\times 1}$ are transmitted and decoded symbol vectors, respectively. From (2), $d^2(\mathbf{y}', \mathbf{y})$ can be expressed as

$$d^2(\mathbf{y}', \mathbf{y}) = ||\bar{\mathbf{D}}\mathbf{F}\mathbf{\Lambda}_{\frac{1}{2N}}\mathbf{\Lambda}_b^{\mathcal{H}}(\mathbf{s}' - \mathbf{s})||^2. \quad (4)$$

Denote $d^2(\mathbf{y}', \mathbf{y}) = ||\bar{\mathbf{D}}\mathbf{e}||^2 = ||\mathbf{D}\mathbf{e}||^2 = ||\mathbf{D}_e\mathbf{h}_f||^2$, where $\mathbf{e} = \mathbf{F}\mathbf{\Lambda}_{\frac{1}{2N}}\mathbf{\Lambda}_b^{\mathcal{H}}(\mathbf{s}' - \mathbf{s})$, and $\mathbf{D}_e = \mathrm{diag}(\mathbf{e})$. The frequency domain channel response $\mathbf{h}_f$ is obtained through the N-point FFT of the length $L+1$ CIR $\mathbf{h}$ as $\mathbf{h}_f = \mathbf{V}_N\mathbf{h}$, where $\mathbf{V}_N = [\mathbf{v}(0), \ldots, \mathbf{v}(N-1)]^T$, $\mathbf{v}(n) = [1, w^n, \ldots, w^{nL}]^T$ with $w = e^{-j2\pi/N}$. Define further $\mathbf{R}_h = \mathcal{E}(\mathbf{h}\mathbf{h}^{\mathcal{H}}) = \mathbf{B}\mathbf{B}^{\mathcal{H}}$ as the $(L+1)\times(L+1)$ channel correlation matrix and the pre-whitened channel vector $\bar{\mathbf{h}} = \mathbf{B}^{-1}\mathbf{h}$, where we assume $\mathbf{B} = \mathbf{R}_h^{\frac{1}{2}}$ is full rank [5]. Therefore, we have

$$d^2(\mathbf{y}', \mathbf{y}) = ||\mathbf{D}_e\mathbf{h}_f||^2 = \bar{\mathbf{h}}^{\mathcal{H}}\mathbf{C}_e\bar{\mathbf{h}}, \quad (5)$$

where $\mathbf{C}_e = \mathbf{B}^{\mathcal{H}}\mathbf{V}_N^{\mathcal{H}}\mathbf{D}_e^{\mathcal{H}}\mathbf{D}_e\mathbf{V}_N\mathbf{B}$.

At high SNR, averaging over all channel realizations in (3) the probability of error follows the expression [2]

$$P(\mathbf{s} \to \mathbf{s}') \leq \left(G_{e,c}\frac{1}{4N_0}\right)^{-G_{e,d}}, \quad (6)$$

where $G_{e,d} = R(\mathbf{C}_e)$ and $G_{e,c}$ are the pairwise multipath diversity and coding gains. Through these pairwise quantities the multipath diversity is defined as

$$G_d = \min_{\forall \mathbf{s}\neq\mathbf{s}'} \quad G_{e,d}. \quad (7)$$

Since $\mathbf{C}_e$ is an $(L+1)\times(L+1)$ matrix, diversity is upper bounded by $R(\mathbf{R}_h)$.

III. Diversity of A-OCDM

We begin our analysis by determining the condition for which A-OCDM system in (2) can enable maximum diversity. We note that if

$$\prod_{k=0}^{N-1} |\boldsymbol{\theta}_k^T(\mathbf{s} - \mathbf{s}')| \neq 0, \forall \mathbf{s} \neq \mathbf{s}' \in \mathbb{Z}(j)^{N\times 1}, \quad (8)$$

where $\boldsymbol{\theta}_k^T$ is the k-th row of $\mathbf{F}\mathbf{\Lambda}_{\frac{1}{2N}}\mathbf{\Lambda}_b^{\mathcal{H}}$, then the system in (2) enables a maximum diversity of $G_d = L+1$ with MLE.

This can be seen from the following: Since $\mathbf{D}_e = \mathrm{diag}(\mathbf{F}\mathbf{\Lambda}_{\frac{1}{2N}}\mathbf{\Lambda}_b^{\mathcal{H}}(\mathbf{s}' - \mathbf{s}))$, if $\boldsymbol{\theta}_k^T(\mathbf{s} - \mathbf{s}') \neq 0$, $\forall k$, implied by (8), then

$$R(\mathbf{D}_e) = R(\mathrm{diag}(\mathbf{F}\mathbf{\Lambda}_{\frac{1}{2N}}\mathbf{\Lambda}_b^{\mathcal{H}}(\mathbf{s}' - \mathbf{s}))) = N.$$

Furthermore, the diversity enabled by A-OCDM is given by $R(\mathbf{B}^{\mathcal{H}}\mathbf{V}_N^{\mathcal{H}}\mathbf{D}_e^{\mathcal{H}}\mathbf{D}_e\mathbf{V}_N\mathbf{B})$. Thus, if $\mathbf{D}_e$ has a full rank of N, a diversity of $G_d = \mathrm{rank}(\mathbf{C}_e) = L+1$ can be enabled.

Therefore, the achievability of maximum diversity for A-OCDM depends on the diagonal matrix $\mathbf{\Lambda}_b$, which in turn depends on the variable b. Fortunately, we can simplify the task of finding optimal b given arbitrary N by formulating it as a precoding problem. There exists a class of unitary precoders $\mathbf{\Theta}$ with the cost constraint $\mathrm{Tr}(\mathbf{\Theta}\mathbf{\Theta}^{\mathcal{H}}) = N$ that can be written in the form $\mathbf{\Theta} = \mathbf{F}\mathbf{D}_\alpha$, where $\mathbf{D}_\alpha = \mathrm{diag}([1, \alpha_1, \alpha_1^2, \ldots, \alpha_1^{N-1}])$ such that diversity and coding gains are maximized when precoding over OFDM transmissions. The design criteria for α_1 are already thoroughly studied and documented [11]. Inspired by this observation, we can

[1] When blocksize N is odd, the transform takes form in a slightly different structure [9].

treat $\mathbf{\Theta} = \mathbf{F}\mathbf{\Lambda}_{\frac{1}{2N}}\mathbf{\Lambda}_b^{\mathcal{H}}$ as a precoder over the diagonalized channel in (2) and design b to enable maximum diversity accordingly.

The following proposition characterizes a set of b such that the resulting A-OCDM system enables the maximum diversity:

Proposition 1: Let $b = \frac{1}{c}, \forall c \in \mathbb{N}$, A-OCDM system in (2) enables maximum diversity with MLE if

$$c \neq \frac{2N(n_1^2 - n_2^2)}{n_1^2 - n_2^2 - 2mN}, \quad \forall n_1, n_2 \in [0, \ldots, N-1], n_1 \neq n_2, m \in \mathbb{Z} \tag{9}$$

Proof: See Appendix A ■

Proposition 1 can be interpreted as follows. We want to find some b such that $\mathbf{F}\mathbf{\Lambda}_{\frac{1}{2N}}\mathbf{\Lambda}_b^{\mathcal{H}}$ serves as an equivalent precoder matrix conforming to the design principles of LCP [12], such that (8) holds. In LCP-OFDM, the diagonal elements of the matrix $\mathbf{D}_\alpha$ are unique, with phases scale linearly with n. However, the phases of diagonal elements of $\mathbf{\Lambda}_{\frac{1}{2N}}\mathbf{\Lambda}_b^{\mathcal{H}}$ have a quadratic dependence on n. Thus, to ensure elements of $\mathrm{diag}(\mathbf{\Lambda}_{\frac{1}{2N}}\mathbf{\Lambda}_b^{\mathcal{H}})$ are unique, b should be chosen to prevent repetitive entries in $\mathrm{diag}(\mathbf{\Lambda}_{\frac{1}{2N}}\mathbf{\Lambda}_b^{\mathcal{H}})$. Inequality constraint on c in (9) ensures uniqueness.

Note that we have not proved the existence of b for arbitrarily large blocksize N. However, practically, for all finite blocksize N, a subset of b satisfying Proposition 1 can be empirically obtained by a linear search. In what follows, we restrict ourselves to the values of b satisfying Proposition 1 such that coding gain can be explored.

In Table I, we provide example values of b based on Proposition 1. Defining $\gamma_k = [\sqrt{N}\mathbf{F}\mathbf{\Lambda}_{\frac{1}{2N}}\mathbf{\Lambda}_b^{\mathcal{H}}]_{k,1}, k \in [0, N-1]$, corresponding entries in equivalent precoder matrices are shown. Without the need for LCP, A-OCDM enables efficient computations and implementations as that of unprecoded OCDM [9].

IV. Numerical Results

We demonstrate i) A-OCDM enables maximum diversity by comparing it against LCP-OCDM in [5] and ii) A-OCDM preserves OCDM's resilience against interference. We use QPSK as modulation and sphere decoder (SD) for equalization, the average BERs is obtained through Monte-Carlo simulations.

Fig. 1 verifies that our design of A-OCDM does indeed enable maximum diversity as LCP-OCDM. For this simulation, we choose $N = 8$, $L = 2$ for a maximum diversity of 3. The LCP-OCDM chooses $\alpha_1 = e^{j\frac{\pi}{2N}} = e^{j\pi\frac{1}{16}}$, which can be designed in the same way as that of OFDM in [11]. We choose $b = \frac{1}{7}$ based on Table II. As a comparison, we have included OCDM system in [9], which enables unit diversity with $b = \frac{1}{2N} = \frac{1}{16}$, and an A-OCDM system with parameter $b = \frac{1}{8}$. As seen in Fig. 1, A-OCDM system with $b = \frac{1}{8}$ fails to achieve maximum diversity. This is because for $N = 8$, $[\mathbf{\Lambda}_{\frac{1}{16}}\mathbf{\Lambda}_{\frac{1}{8}}^{\mathcal{H}}]_{1,1} = [\mathbf{\Lambda}_{\frac{1}{16}}\mathbf{\Lambda}_{\frac{1}{8}}^{\mathcal{H}}]_{5,5}$, elements of $\mathrm{diag}([\mathbf{\Lambda}_{\frac{1}{16}}\mathbf{\Lambda}_{\frac{1}{8}}^{\mathcal{H}}])$ are not unique, thus $b = \frac{1}{8}$ does not satisfy Proposition 1 and A-OCDM system with $b = \frac{1}{8}$ do not enable maximum diversity.

One of the main advantages of OCDM is its robustness against NBIs offered by spreading. We choose to model the NBI and employ frequency domain minimum mean square error (MMSE) equalizer from [13]. We choose blocksize $N = 256$, $L + 1 = 4$ and the number of effective interferers $N_{\mathcal{A}} = 8, 32$. To enable maximum diversity, we choose $b = \frac{1}{129}$. Unsurprisingly, A-OCDM exhibits identical performance as OCDM, due to having the same chirp rate of $\frac{1}{2N}$. Furthermore, in Fig. 2, the BER curves for OCDM-based systems reach the lowest points at around 20 dB SNR. This pattern is due to low SNR region dominated by noise and high SNR region dominated by interference, and we note that similar observations are present in [4] and [13].

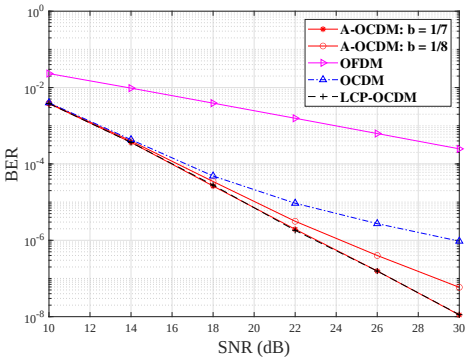

Fig. 1: BER performance of OCDM, LCP-OCDM and A-OCDM with variable basis

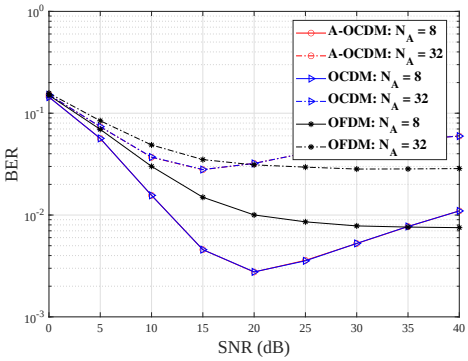

Fig. 2: Performance of A-OCDM against interference with MMSE

Remark 2: A-OCDM preserves a number of other properties possessed by OCDM systems in [9]. For instance, it can be shown that both systems share identical distribution of peak to average power ratio (PAPR), similar mutual information (MI), and same LE performance, as also implied from Fig. 2.

Appendix A: Proof of Proposition 1

Our approach in this proof is based on LCP. Accordingly, we draw on the extensive literature on algebraic number theory, and readers may consult [3], [12] and [14] for more detailed expositions.

We rely on the following definitions: $\mathbb{Q}(j)$ is a subfield of $\mathbb{C}$ that includes both $\mathbb{Q}$ and j, and $\mathbb{Q}(j)[\alpha]$ is an extension field of $\mathbb{Q}$ by adjoining α to the field of $\mathbb{Q}(j)$.

Let $b \in \mathbb{R}$, where $b = \frac{1}{c}$ for some $c \in \mathbb{N}$. Define $\lambda_n = [\mathbf{\Lambda}_{\frac{1}{2N}}\mathbf{\Lambda}_b^{\mathcal{H}}]_{n,n}$. Then by the definition of cyclotomic field [12,

TABLE I: Design Examples of $\sqrt{N}\mathbf{F}\mathbf{\Lambda}_{\frac{1}{2N}}\mathbf{\Lambda}_b^{\mathcal{H}}$ Based on Blocksize N

N	b	γ_0	γ_1	γ_2	γ_3	γ_4	γ_5	γ_6	γ_7
2	$\frac{1}{3}$	$e^{-j\frac{\pi}{6}}$	$e^{-j\frac{7\pi}{6}}$						
3	$\frac{1}{4}$	$e^{-j\frac{\pi}{6}}$	$e^{-j\frac{5\pi}{6}}$	$e^{-j\frac{9\pi}{6}}$					
4	$\frac{1}{3}$	$e^{-j\frac{5\pi}{12}}$	$e^{-j\frac{11\pi}{12}}$	$e^{-j\frac{17\pi}{12}}$	$e^{-j\frac{23\pi}{12}}$				
5	$\frac{1}{3}$	$e^{-j\frac{7\pi}{15}}$	$e^{-j\frac{13\pi}{15}}$	$e^{-j\frac{19\pi}{15}}$	$e^{-j\frac{25\pi}{15}}$	$e^{-j\frac{31\pi}{15}}$			
6	$\frac{1}{5}$	$e^{-j\frac{7\pi}{30}}$	$e^{-j\frac{17\pi}{30}}$	$e^{-j\frac{27\pi}{30}}$	$e^{-j\frac{37\pi}{30}}$	$e^{-j\frac{47\pi}{30}}$	$e^{-j\frac{57\pi}{30}}$		
7	$\frac{1}{5}$	$e^{-j\frac{9\pi}{35}}$	$e^{-j\frac{19\pi}{35}}$	$e^{-j\frac{29\pi}{35}}$	$e^{-j\frac{39\pi}{35}}$	$e^{-j\frac{49\pi}{35}}$	$e^{-j\frac{59\pi}{35}}$	$e^{-j\frac{69\pi}{35}}$	
8	$\frac{1}{7}$	$e^{-j\frac{9\pi}{56}}$	$e^{-j\frac{23\pi}{56}}$	$e^{-j\frac{37\pi}{56}}$	$e^{-j\frac{51\pi}{56}}$	$e^{-j\frac{65\pi}{56}}$	$e^{-j\frac{79\pi}{56}}$	$e^{-j\frac{93\pi}{56}}$	$e^{-j\frac{107\pi}{56}}$

D1] , we see that λ_n belongs to the $2Nc$-th cyclotomic field as

$$\lambda_n = e^{j2\pi\frac{(c-2N)n^2}{2Nc}} \in \mathbb{Q}(j)[e^{j2\pi\frac{1}{2Nc}}] \qquad n \in [0,\dots,N-1]. \tag{10}$$

Let $\gamma_{k,1}$ be the root of a minimum monic polynomial $p(x)$ over $\mathbb{Q}(j)$, where $\gamma_{k,n} = \lambda_n\beta_k^n$ and $\beta_k = e^{j2\pi k/N}$. In an explicit form, $\gamma_{k,n}$ is defined as

$$\gamma_{k,n} = e^{-j2\pi kn/N}e^{j2\pi\frac{(c-2N)n^2}{2Nc}} = [\sqrt{N}\mathbf{F}\mathbf{\Lambda}_{\frac{1}{2N}}\mathbf{\Lambda}_b^{\mathcal{H}}]_{k,n}. \tag{11}$$

Symbols $\gamma_{k,n}, k, n \in [0,\dots,N-1]$ are elements of the $2Nc$-th cyclotomic field. We note that an element is integral over $\mathbb{Z}(j)$ if it is a root of a monic polynomial with coefficient in $\mathbb{Z}(j)$ [12, D4]. By definition, cyclotomic polynomial has only integer coefficients and hence elements of a cyclotomic field are all integral over $\mathbb{Z}(j)$. Assume for now that elements of $\boldsymbol{\theta}_1^T$ are linearly independent, where $\boldsymbol{\theta}_k^T$ is the k-th row of $\mathbf{\Theta} = \mathbf{F}\mathbf{\Lambda}_{\frac{1}{2N}}\mathbf{\Lambda}_b^{\mathcal{H}}$. Given that $\mathbf{s}-\mathbf{s}' \in \mathbb{Z}(j)^{N\times 1}$, we can establish that $\boldsymbol{\theta}_1^T(\mathbf{s}-\mathbf{s}')$ is integral over $\mathbb{Z}(j)$. Define the cyclotomic field $\mathbb{Q}(j)[\gamma]$, where $\gamma = e^{j2\pi\frac{1}{2Nc}}$ from (10) [12, D1]. Then it follows that $\mathbf{\Theta} \in \mathbb{Q}(j)[\gamma]^{N\times N}$. For $N = 2^z, z \in \mathbb{N}$, the Euler totient number of $2Nc$ is at least N. Hence, $\deg(\mathbb{Q}(j)[\gamma]) \geq N$, we define $\eta_k, k = [0,\dots,N-1]$ as N distinct $\mathbb{Q}(j)$-isomorphisms of $\mathbb{Q}(j)[\gamma]$ such that $\eta_k(\gamma_{0,1}) = \gamma_{k,1}, \forall n$ [3] [12, D3]. To facilitate further proof, we define

$$f(\gamma_k) = \left|\frac{1}{\sqrt{N}}\sum_{n=0}^{N-1}\gamma_{k,n}(s_l - s_l')\right|, \tag{12}$$

then the product distance in (8) can be written as

$$\begin{aligned}\mathcal{N}(f(\gamma_0)) &= \prod_{k=0}^{N-1}\eta_k\left(\left|\frac{1}{\sqrt{N}}\sum_{n=1}^{N}\gamma_{0,n}(s_l - s_l')\right|\right)\\ &= \prod_{k=0}^{N-1}\left|\frac{1}{\sqrt{N}}\sum_{n=0}^{N-1}(\gamma_{k,n}(s_l - s_l'))\right|\\ &= \prod_{k=0}^{N-1} f(\gamma_k) \overset{(\alpha)}{\neq} 0, \quad \forall \mathbf{s} \neq \mathbf{s}' \in \mathbb{Z}(j)^{N\times 1},\end{aligned} \tag{13}$$

where s_l, s_l' are the l-th elements of $\mathbf{s}$, $\mathbf{s}'$, respectively. (α) in (13) follows from the result in [12, Appendix H]. There remains but one question, (α) in (13) relies on our assumption that elements of $\boldsymbol{\theta}_1^T, \gamma_{0,n}, n = [0,\dots,N-1]$ constitute unique coordinates over the ring of Gaussian integers. However, unlike the LCP used in [2], where elements of $\mathbf{D}_\alpha$ form a basis over $\mathbb{Q}(j)$, our definition of $\gamma_{k,n}$ entails a quadratic dependence of phase on n. Hence for $n_1 \neq n_2$, $\gamma_{k,n_1} = \gamma_{k,n_2}$ is possible. In other words, depending on the choice of c, it is possible for $\gamma_{0,n}, n = [0,\dots,N-1]$ to be an overlapping subset of the basis of $\mathbb{Q}(j)[\gamma]$ over $\mathbb{Q}(j)$. Thus, we need to enforce $\gamma_{0,n}, n = [0,\dots,N-1]$ are distinct. Explicitly, we have

$$\gamma_{0,n} = e^{j2\pi\frac{(c-2N)n^2}{2Nc}}, \tag{14}$$

where N distinct $\gamma_{0,n}$ exist if and only if

$$(c-2N)n_1^2 - 2Ncm \neq (c-2N)n_2^2, \tag{15}$$

for $n_1 \neq n_2,\ n_1, n_2 \in [0,\dots,N-1]$ and $m \in \mathbb{Z}$. Expanding the expression in (15) and rearranging terms results in the form presented in Proposition 1.

REFERENCES

[1] J. Boutros and E. Viterbo, "Signal space diversity: A power and bandwidth-efficient diversity technique for the Rayleigh fading channel," *IEEE Trans. Inf. Theory*, vol. 44, no. 4, pp. 1453–1467, Jul. 1998.

[2] Z. Liu, Y. Xin, and G. B. Giannakis, "Linear constellation precoding for OFDM with maximum multipath diversity and coding gains," *IEEE Trans. Commun.*, vol. 51, no. 3, pp. 416–427, Mar. 2003.

[3] J. Boutros, E. Viterbo, C. Rastello, and J.-C. Belfiore, "Good lattice constellations for both Rayleigh fading and Gaussian channels," *IEEE Trans. Inf. Theory*, vol. 42, no. 2, pp. 502–518, Mar. 1996.

[4] M. S. Omar and X. Ma, "Performance analysis of OCDM for wireless communications," *IEEE Trans. Wireless Commun.*, vol. 20, no. 7, pp. 4032–4043, Jul. 2021.

[5] ——, "Designing OCDM-based multi-user transmissions," in *Proc. IEEE Glob. Commun. Conf.*, Waikoloa, USA, Dec. 2019, pp. 1–6.

[6] M. Martone, "A multicarrier system based on the fractional Fourier transform for time-frequency-selective channels," *IEEE Trans. Commun.*, vol. 49, no. 6, pp. 1011–1020, Jun. 2001.

[7] T. Erseghe, N. Laurenti, and V. Cellini, "A multicarrier architecture based upon the affine Fourier transform," *IEEE Trans. Commun.*, vol. 53, no. 5, pp. 853–862, May. 2005.

[8] A. Bemani, N. Ksairi, and M. Kountouris, "AFDM: A full diversity next generation waveform for high mobility communications," in *Proc. IEEE Int. Conf. Commun. Workshops*, Montreal, Canada, Jun. 2021, pp. 1–6.

[9] X. Ouyang and J. Zhao, "Orthogonal chirp division multiplexing," *IEEE Trans. Commun.*, vol. 64, no. 9, pp. 3946–3957, Sep. 2016.

[10] Z. Wang and G. B. Giannakis, "Wireless multicarrier communications," *IEEE Signal Process. Mag.*, vol. 17, no. 3, pp. 29–48, May. 2000.

[11] X. Ma and G. B. Giannakis, "Complex field coded MIMO systems: performance, rate, and trade-offs," *Wirel. Commun. Mob. Comput.*, vol. 2, no. 7, pp. 693–717, Nov. 2002.

[12] Y. Xin, Z. Wang, and G. B. Giannakis, "Space-time diversity systems based on linear constellation precoding," *IEEE Trans. Wireless Commun.*, vol. 2, no. 2, pp. 294–309, Mar. 2003.

[13] M. S. Omar and X. Ma, "The effects of narrowband interference on OCDM," in *Proc. IEEE Int. Workshop Signal Process. Adv. Wireless Commun.*, Atlanta, USA, May. 2020, pp. 1–5.

[14] D. A. Marcus, *Number Fields*. New York, NY: Springer-Verlag, 1977.